PASJ: Publ. Astron. Soc. Japan **51**, 23–37 (1999)

Analysis of the Photospheric Lines of the Magnetic CP Star HR 7575

Ken-ichi Kato
Osaka Science Museum, Nakanoshima, Kita-ku, Osaka 530-0005
E-mail (KK): kato@sci-museum.kita.osaka.jp
and
Kozo Sadakane
Astronomical Institute, Osaka Kyoiku University, Asahigaoka, Kashiwara, Osaka 582-8582

(Received 1997 August 4; accepted 1998 November 18)

Abstract

The photospheric lines in the visual region of the cool magnetic CP star HR 7575 have been analyzed using a high-dispersion spectrogram obtained at the Dominion Astrophysical Observatory. The fully line-blanketed ATLAS9 model atmospheres of 10-times the solar metal content were employed to calculate the elemental abundances. The effective temperature T_{eff}, derived from the optical and ultraviolet energy distributions, points to 8500 ± 300 K, while the ionization balance of iron is not reproduced at this effective temperature. The abundances derived from individual Cr I, Cr II, and Fe II lines apparently depend on their effective Landé factors. This implies that the Cr and Fe lines are intensified by the strong magnetic field on HR 7575. Their abundance enhancement is estimated to be about 0.7 dex based on a computation of the Unno–Beckers equation. The overall abundance patterns of HR 7575 are comparable to other cool magnetic CP stars. Of the analyzed elements, only Mg and Sc have nearly solar abundances, while Cr, Mn, Sr, and rare earths are overabundant by 1 to 5 dex.

Key words: Abundances — Stars: individual (HR 7575) — Stars: magnetic — Stars: peculiar A

1. Introduction

It is generally accepted that magnetic chemically peculiar stars [CP2 stars, in the classification of Preston (1974)] consist of two groups of different effective temperatures: a cooler one which shows an enhancement of elements such as Cr, Sr, and Eu, and a warmer group which exhibits an unusual strength of Si lines. Their spectroscopic properties and peculiarities of elemental abundances have been summarized in a number of papers, such as Preston (1974), Wolff (1983), Adelman and Cowley (1986), Ryabchikova (1991), and Cowley (1993).

HR 7575 (HD 188041 = V1291 Aql) is a cool magnetic CP star with an exceptionally long period of light variation of about 224 days among these stars (Babcock 1960; Wolff 1969). In his catalogue, Osawa (1965) noted its spectral feature as "Sr Cr Eu strong, hydrogen spectral type : A2, and metallic type : F2". A major photometric property of HR 7575 is its very large m_1 value, defined as $m_1 = (v - b) - (b - y)$. Therefore, it is clearly recognizable on the c_1– m_1 plane from other stars, including normal, Am, and Ap stars (Warren 1973).

The four-color photometry by Jones and Wolff (1973) showed that at a phase of $P = 0.45$ (corresponds to the maximum phase of the magnetic field) the v mag (around 4100 Å) drops by 0.1 mag, the variation in the u-band (around 3500 Å) is very small, and there is no change in the b-band (around 4700 Å), while the V mag (around 5400 Å) increases by 0.02 mag. This phenomenon can be seen more clearly in the ten-color photometry of Musielok et al. (1980). That is, the "null wavelength region" is present between 4500 Å and 5000 Å, and the light at the blue portion varies in antiphase with that at a longer wavelength range. This is usually interpreted as an effect of the variable backwarming of radiation due to line-blanketing, which results in a redistribution of radiation from the ultraviolet to the visual region (Kodaira 1967, 1973; Jones, Wolff 1973; Schöneich 1981). In addition, a change in the β-index is also observed. It shows a minimum at a phase of 0.4, and a maximum at a phase of 0.9; this change is in synchronization with the variation of V mag (Musielok 1986a, 1986b; Musielok, Madej 1988).

The magnetic field of HR 7575 was first detected by Babcock (1954, 1958). After his pioneering study, a number of authors have attempted to measure the magnetic field and related spectroscopic phenomena on HR 7575. We can find several measurements of the strength in the catalogue of Didelon (1983), such as −230–+1470 Gauss, +4000 G, and +350–+1270 G. Preston (1971) has reported a mean surface magnetic field of up to 4600 G based on observations of Cr and Fe line features broadened by the Zeeman effect. Mathys (1990) succeeded to display that the Fe I line at 6149.24 Å has a fully resolved Zeeman pattern, from which he determined the strength of the magnetic field to be 3300 G (Mathys, Lanz 1992). Moreover, Mathys (1991) has obtained some different mean longitudinal magnetic fields of 905–1850 G from the polarization of Cr and Fe lines. The magnetic field on HR 7575 is also known to vary at the period of light variation (Babcock 1960; Wolff 1969; Catalano, Renson 1984; Mathys 1991). It has been shown by Jones and Wolff (1973) that the line strengths of rare earths and iron-group elements slightly increase at a phase of a stronger magnetic field. These magnetic and spectroscopic properties strongly suggest that HR 7575 has a non-uniform distribution of some elements over the surface. However, we can find no literature to show explicitly the presence of such spots of elements.

Spectral-line identifications were made by Hartoog et al. (1973) using the wavelength coincidence statistics (WCS) method; they found the so-called Nd–Sm anomaly, a phenomenon that lines of Nd and Sm are not successfully detected, while other rare earth elements such as Eu, Ce, and Gd show unusually strong features (Cowley 1976, 1977, 1979a; Cowley, Aikman 1980). Spectral lines of heavy elements in HR 7575 have been systematically investigated by Cowley and his colleagues: Cowley (1976) for Y, Ba, and lanthanides, Cowley (1977) for Pt, Cowley et al. (1977) for U and Th lines, and Cowley (1979b) for V and other metals. A very strong feature of Li I at 6708 Å was found by Faraggiana et al. (1986). In the ultraviolet spectra taken by the IUE satellite, Faraggiana (1989) identified Pb lines, although no features of Th and U were found. Mathys and Cowley (1992) have detected a line of doubly ionized praseodymium (Pr III) at 6160.2 Å. A systematic line-by-line identification for 1243 lines was performed by Kato and Sadakane (1993) in the spectral range from 4200 Å to 4600 Å.

Elemental abundance analyses were made by Allen (1977) for Fe, Sr, Y, and Zr, and Allen and Cowley (1977) for Cr, Mn, and Fe. They concluded that the abundances of Fe and Y are solar, and Cr, Mn, and Zr are overabundant by 1 to 2 dex. However, these abundance results seem to be fairly moderate because other cool magnetic CP stars show higher abundances up to 5 dex (these large values are obtained without taking into account the influence of magnetic intensification or hyperfine-structure splitting). As noted above, HR 7575 has a very large m_1 value compared with that of other magnetic stars, which suggests that line blanketing due to more abundant metals is very significant. Therefore, a fine analysis using recent fully line-blanketed model atmospheres is desirable to explore the abundance property of this cool magnetic CP star. In this paper, we discuss the abundance analysis for HR 7575 using Kurucz's (1993a) ATLAS9 model atmospheres and the effect of the magnetic field to the spectral lines. Some fundamental data for HR 7575 are summarized in table 1.

Table 1. Fundamental data for HR 7575 = HD 188041 = V1291 Aql.

Characteristics		Ref
Spectral type	A5p	1
	F0pSrCrEu	4
V	5.65	1
$B-V$	0.20	1
$U-B$	0.10	1
$b-y$	0.051	2
m_1	0.313	2
c_1	0.773	2
β	2.850	2
$v \sin i$	2 km s^{-1}	1
Magnetic field	-230–$+1470$	3
Variability in V	5.61–5.67	1
Period	224 d	1

Reference: 1. Hoffleit (1982); 2. Hauck, Mermilliod (1980); 3. Babcock (1958); 4. Buscombe (1977).

2. Spectrogram and Line Selection

We used a high-dispersion spectrogram (2.4 Å mm^{-1}, plate number 9483) obtained at the Dominion Astrophysical Observatory (DAO) at Modified Julian Date = 42350.1299, which corresponds to a phase of 0.67 (based on Jones and Wolff 1973) or 0.77 (based on Mathys 1991) after the maximum of the magnetic field. This is the same material as that employed in analyses by Cowley (1976), Allen (1977), and Allen and Cowley (1977). The spectrogram was digitized using a PDS machine during the stay of one of the authors (K. S.) at the DAO in 1990. It covers the spectral region from 4194 Å to 4602 Å, from which we measured the equivalent widths of 1243 lines. The details concerning line identification are presented in Kato and Sadakane (1993). We selected clean lines suitable for an abundance computation during the line identification. Some contaminated lines of the key elements, such as Mg II and Eu II, were also included, if necessary. All of the equivalent widths were measured using the data-processing software package IRAF (Image Reduction and Analysis Facility, distributed by the National Optical Astronomy Observatories) with the help of the spectral data-analysis tool *Nijiboshi* (it means stars with rainbow colors) developed by J. Katahira and T. Hasui to be used on personal computers.

In a previous study (Kato, Sadakane 1993), the equivalent widths were evaluated using the gf values cited in the ATMLINE database (Horaguchi, Hirata 1989) for a total of 20670 lines in the corresponding wavelength range. We have found that the input elemental abundances should be increased by 0.3 to 5 dex from the solar values to reproduce the observed equivalent widths. Finally, 93% of the lines with their equivalent width of $W_\lambda \geq 50$ mÅ were possibly identified. The following atomic species have clean lines: Ca I, Sc II, Ti II, Cr I, Cr II, Mn I, Mn II, Fe I, Fe II, Ni I, La II, Ce II, Pr II, Eu II, and Gd II. However, we have failed to confirm the identification of the Mo II lines (cf, Cowley 1993).

It is extremely difficult to place the continuum level, because its spectrum is crowded with so many strong absorption lines. The mean line density is 3.1 lines Å^{-1}. This should be compared with 2.3 lines Å^{-1} for the lower temperature star Procyon (F5 IV–V). Therefore, the measured equivalent widths may be subject to large errors. The selected lines and their equivalent widths are presented in table 2.

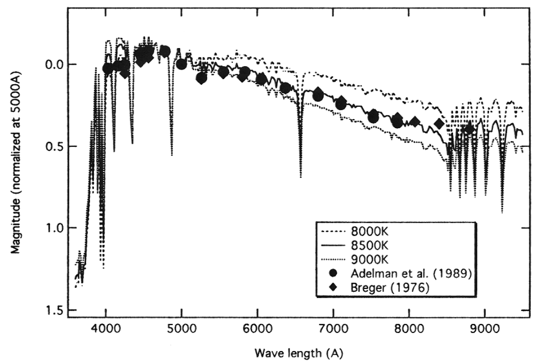

Fig. 1. Comparison of the observed and model fluxes of HR 7575. The flux units are magnitudes normalized to zero at 5000 Å. The observed fluxes are taken from Breger (1976) and Adelman et al. (1989).

3. Model Parameters

The flux data, colors, and Hγ line profiles are used to derive the effective temperature $T_{\rm eff}$ and the surface gravity $\log g$, where Kurucz's (1993a) ATLAS9 model atmospheres of 10-times the solar metal content are employed.

3.1. *Continuum Fluxes and Colors*

We compare in figure 1 the observed Paschen continuum fluxes (Breger 1976; Adelman et al. 1989) and the model flux distributions for $\log g = 3.5$, both of which are normalized at 5000 Å. We can find dips of fluxes at 4200 Å ($1/\lambda = 2.38$) and at 5200 Å ($1/\lambda = 1.92$), and a weak dip at 6300 Å ($1/\lambda = 1.59$). Such an unusual flux distribution appears in the spectra of many cool CP stars (e.g., Adelman 1981). Since model fluxes for the solar abundance atmospheres show no distinct dip at around 5200 Å ($1/\lambda = 1.92$), these features are expected to reflect the selective absorption by metallic lines (Adelman, Cowley 1986; Lebedev 1987). From the comparison in figure 1, we obtain $T_{\rm eff} = 8600$ K for the flux distribution at longward of λ 6000 Å, and $T_{\rm eff} = 8200$ K for the blue portion. Finally, we estimate $T_{\rm eff} = 8500 \pm 300$ K. We examined two cases for the surface gravity of $\log g = 3.5$ and 4.0, and found that the model fluxes are insensitive to the choice of the surface gravity.

We tried to determine the effective temperature from the color indices by taking the unusual continuum fluxes of HR 7575 into account. Here, we assume $\log g = 3.5$, because the flux distributions and, resultantly, colors are weakly dependent on the surface gravity, as shown above. Based on a calibration by Lester et al. (1986) for 10-times the solar composition, $T_{\rm eff} = 7950$ K can be derived from $b - y = 0.051$ (Hauck, Mermilliod 1980) and $T_{\rm eff} = 8010$ K from $b - y = 0.046$ (Warren 1973). Smalley and Dworetsky's (1995) calibration for the β-index indicates $T_{\rm eff} = 8100$ K. Empirical $T_{\rm eff}$–*uvby* relations for magnetic CP stars constructed from effective temperatures obtained by many spectroscopists (Mégessier 1988; Shallis, Blackwell 1979; Shallis et al. 1985; Stępień, Dominiczak 1989) point to $T_{\rm eff} = 8200$ K. The color measurements by Hauck and North (1982) in the Geneva system for HR 7575 were converted to effective temperature by the formula of Hauck and North (1993). This yields $T_{\rm eff} = 8100$ K. From these photometries, $T_{\rm eff} = 8070 \pm 200$ K is concluded.

Ultraviolet flux measurements by the TD1 (Thompson et al. 1978) and the ANS (Wesselius et al. 1982) satellites are available for HR 7575. To establish an empirical relation between the flux ratios [f(1565 Å)/f(1965 Å), f(1565 Å)/f(2365 Å)] measured by the TD1 satellite and effective temperatures, we employed empirical temperatures of magnetic stars determined by Mégessier (1988), Shallis and Blackwell (1979), Shallis et al. (1985), and Stępień and Dominiczak (1989). We found both the flux ratios f(1565 Å)/f(1965 Å) and f(1565 Å)/f(2365 Å) to be fairly sensitive to the effective temperature between 8000 K and 9500 K. A comparison of the data of HR 7575 [f(1565 Å)/f(1965 Å) = 0.32 and f(1565 Å)/f(2365 Å) = 0.39] indicates $T_{\rm eff} = 8700 \pm 200$ K. Figure 2 displays the ultraviolet flux distributions in magnitude for five bands centered on 15, 18, 22, 25, and 33 nm as well as for other magnetic stars measured by the ANS. The flux pattern of HR 7575 is quite similar to that of HD 204411 ($T_{\rm eff} = 8750$ K, Shallis et al. 1985), except for band 18. Thus, we obtain $T_{\rm eff} = 8700 \pm 200$ K from ultraviolet fluxes.

3.2. Hγ *Line Profiles*

Figure 3 represents the Hγ line profiles measured on the intensity tracings and theoretically evaluated profiles for $\log g = 3.5$ using the *unified theory* of Vidal

Table 2. Data for the lines used in the analysis.

Element Solar ε	λ (Å)	χ (eV)	$\log gf$	$\log g_{\rm rad}$	$\log C_4$	$\log C_6$	W_λ (mÅ)	Weight	$\log \varepsilon$ adopted	$\log \varepsilon$ 9500 K
Mg II										
$\log \epsilon_\odot$	4481.23	8.864	0.970	6.90	−13.01	0.76	441	1	7.59	7.77
= 7.58									⟨7.59⟩	⟨7.77⟩
Ca I										
$\log \epsilon_\odot$	4226.73	0.000	0.240	8.26	−14.36	1.25	135	2	6.34	7.72
= 6.36	4302.50	1.899	0.280	0	0	1.25	118	2	7.25	8.51
	4425.44	1.879	−0.360	8.26	−14.26	1.25	72	4	6.96	8.18
	4454.78	1.899	0.260	0	0	−29.84	143	2	7.76	9.03
	4578.55	2.521	−0.697	0	0	1.25	52	3	7.41	8.57
									⟨7.14⟩	⟨8.38⟩
Sc II										
$\log \epsilon_\odot$	4314.08	0.618	−0.100	0	0	0	66	1	2.66	3.35
= 3.1	4415.54	0.595	−0.640	0	0	0.43	74	2	3.29	3.99
									⟨3.08⟩	⟨3.78⟩
Ti II										
$\log \epsilon_\odot$	4277.53	4.968	−0.825	0	0	1.00	35	2	6.12	6.42
= 4.99	4301.92	1.160	−1.160	0	0	0.57	128	3	5.70	6.29
	4394.02	1.221	−1.590	0	0	0.57	87	5	5.27	5.84
	4395.00	1.084	−0.660	8.18	0	0.57	136	4	5.27	5.87
	4395.83	1.242	−2.170	0	0	0.57	82	4	5.77	6.34
	4398.25	1.224	−2.121	0	0	0.57	59	5	5.33	5.88
	4417.71	1.164	−1.430	0	0	0.57	131	5	5.99	6.59
	4418.30	1.236	−2.460	0	0	0.57	87	4	6.14	6.72
	4421.94	2.061	−1.770	0	0	0.57	87	2	6.03	6.55
	4464.46	1.160	−2.080	0	0	0.57	105	1	6.07	6.67
	4468.51	1.130	−0.600	8.08	0	0.57	138	4	5.27	5.88
	4469.11	1.084	−2.869	0	0	1.00	67	2	6.09	6.67
	4470.83	1.164	−2.280	0	0	0.57	96	5	6.09	6.66
	4529.48	1.571	−2.030	0	0	1.00	109	2	6.37	6.93
	4544.01	1.242	−2.400	0	0	1.00	68	1	5.74	6.31
	4563.77	1.221	−0.960	0	0	1.00	143	4	5.77	6.38
	4568.31	1.224	−2.650	0	0	1.00	43	3	5.58	6.14
	4583.40	1.164	−2.720	0	0	1.00	72	4	6.07	6.64
									⟨5.76⟩	⟨6.33⟩
Cr I										
$\log \epsilon_\odot$	4206.89	4.617	0.256	0	0	1.00	50	3	7.85	8.59
= 5.67	4262.38	3.079	−1.230	0	0	1.00	26	5	7.91	8.73
	4275.97	3.878	−0.180	0	0	1.00	62	2	7.98	8.77
	4374.15	3.000	−0.488	0	0	1.00	94	3	8.33	9.20
	4381.11	2.708	−1.050	0	0	1.00	81	3	8.46	9.34
	4384.97	1.030	−1.150	0	0	1.00	96	3	7.73	8.74
	4397.25	3.011	−1.060	0	0	1.00	55	3	8.20	9.04
	4410.30	3.012	−1.010	0	0	1.00	65	2	8.32	9.16
	4413.86	3.550	−0.400	0	0	1.00	67	4	8.02	8.83
	4425.12	3.104	−1.955	0	0	1.00	17	4	8.40	9.22
	4459.73	3.013	−0.650	0	0	1.00	61	5	7.88	8.73
	4462.77	3.010	−1.300	0	0	1.00	26	1	7.92	8.75
	4473.78	2.707	−1.206	0	0	1.00	53	2	8.11	8.97
	4492.31	3.375	−0.392	0	0	1.00	60	5	7.84	8.65

Table 2. (Continued.)

Element Solar ε	λ (Å)	χ (eV)	$\log gf$	$\log g_{\rm rad}$	$\log C_4$	$\log C_6$	W_λ (mÅ)	Weight	$\log\varepsilon$ adopted	$\log\varepsilon$ 9500 K
	4496.86	0.941	−1.150	0	0	1.00	101	4	7.75	8.78
	4501.78	2.915	−1.040	0	0	1.00	52	2	8.06	8.91
	4540.50	2.544	−0.487	0	0	1.00	75	2	7.66	8.56
	4540.71	3.104	0.028	0	0	1.00	100	2	7.98	8.85
	4543.74	2.982	−1.560	0	0	1.00	28	1	8.19	9.03
	4575.12	3.369	−0.970	0	0	1.00	37	1	8.03	8.84
	4578.33	3.849	−0.860	0	0	1.00	21	1	7.86	8.64
	4590.48	4.489	−0.865	0	0	1.00	23	2	8.36	9.10
	4599.00	3.092	−1.619	0	0	1.00	20	1	8.14	8.96
									⟨8.03⟩	⟨8.88⟩
Cr II										
$\log\epsilon_\odot$	4207.35	3.826	−2.475	0	0	1.00	108	2	7.68	8.04
= 5.67	4211.08	5.329	−3.450	0	0	1.00	62	1	8.69	8.92
	4222.00	5.662	−1.927	0	0	1.00	57	4	7.29	7.50
	4224.85	5.329	−1.726	0	0	0.61	91	5	7.55	7.79
	4252.62	3.858	−2.018	0	0	0.61	134	4	7.82	8.20
	4275.57	3.858	−1.709	0	0	0.61	142	5	7.67	8.03
	4277.31	8.350	−1.445	0	0	1.00	46	2	8.27	8.31
	4284.21	3.853	−1.864	0	0	0.61	126	2	7.49	7.85
	4303.56	5.871	−2.283	0	0	1.00	96	2	8.54	8.76
	4306.91	5.873	−1.185	0	0	1.00	91	4	7.35	7.57
	4424.86	11.747	−0.121	0	0	1.00	29	2	8.47	8.35
	4474.56	5.493	−2.076	0	0	1.00	63	3	7.43	7.67
	4503.55	5.662	−3.298	0	0	1.00	32	1	8.21	8.40
	4504.55	3.103	−4.234	0	0	1.00	57	2	7.91	8.30
	4523.45	6.487	−3.136	0	0	1.00	51	4	8.91	9.07
	4531.82	8.362	−1.186	0	0	1.00	62	4	8.33	8.39
	4546.62	7.772	−1.179	0	0	1.00	74	4	8.18	8.29
	4577.42	8.348	−1.420	0	0	1.00	44	2	8.22	8.27
	4587.26	6.487	−1.650	0	0	1.00	76	4	7.89	8.06
	4592.09	4.073	−1.220	0	0	1.00	172	5	7.77	8.14
									⟨7.91⟩	⟨8.13⟩
Mn I										
$\log\epsilon_\odot$	4502.22	2.919	−0.345	0	0	0	59	4	6.98	7.87
= 5.39									⟨6.98⟩	⟨7.87⟩
Mn II										
$\log\epsilon_\odot$	4200.28	6.184	−1.741	0	0	0	43	4	7.11	7.26
= 5.39	4239.18	5.369	−2.250	0	0	0	59	3	7.39	7.61
	4244.24	5.373	−2.396	0	0	0	70	4	7.74	7.98
	4283.77	5.373	−2.204	0	0	0	62	3	7.40	7.62
	4317.71	6.913	−1.917	0	0	0	56	3	7.98	8.10
	4365.22	6.573	−1.350	0	0	0	63	1	7.33	7.47
	4385.73	5.436	−3.029	0	0	0	31	3	7.70	7.89
	4441.99	5.472	−2.355	0	0	0	50	4	7.40	7.60
	4445.90	5.472	−2.856	0	0	0	33	3	7.59	7.78
	4518.96	6.645	−1.329	0	0	0	52	2	7.15	7.29
	4519.24	5.397	−2.567	0	0	0	42	2	7.42	7.63
									⟨7.49⟩	⟨7.68⟩

Table 2. (Continued.)

Element Solar ε	λ (Å)	χ (eV)	$\log gf$	$\log g_{\rm rad}$	$\log C_4$	$\log C_6$	W_λ (mÅ)	Weight	$\log\varepsilon$ adopted	$\log\varepsilon$ 9500 K
Fe I										
$\log\epsilon_\odot$	4202.02	1.485	−0.708	7.91	−13.40	−32.49	102	5	7.62	8.61
= 7.51	4219.36	3.573	0.120	8.15	−13.40	−31.06	85	5	7.84	8.69
	4220.34	3.071	−1.290	8.18	−13.40	−31.28	43	2	8.20	9.05
	4222.21	2.449	−0.967	8.02	−13.26	−30.28	70	3	7.91	8.82
	4225.45	3.417	−0.500	8.33	−13.40	−30.13	76	1	8.20	9.04
	4225.95	3.046	−1.390	0	0	1.00	50	1	8.42	9.27
	4233.60	2.482	−0.604	8.05	−13.22	−29.87	120	3	8.45	9.38
	4248.22	3.071	−1.320	8.21	−13.40	−31.28	68	2	8.64	9.51
	4250.11	2.468	−0.405	8.02	−13.40	−30.10	120	4	8.28	9.22
	4250.78	1.557	−0.710	7.90	−13.40	−31.11	150	4	8.45	9.43
	4300.82	3.984	−1.190	0	0	1.00	47	2	8.77	9.56
	4309.37	2.948	−1.180	0	0	1.00	67	2	8.43	9.30
	4310.37	3.928	−1.500	0	0	1.00	46	2	9.03	9.83
	4382.76	3.573	−1.440	8.08	−13.40	−29.85	46	1	8.72	9.54
	4383.54	1.484	0.200	7.85	−13.40	−31.36	156	3	7.54	8.53
	4388.40	3.602	−0.590	8.08	−13.40	−30.00	93	4	8.70	9.56
	4401.28	3.602	−0.920	0	0	1.00	63	3	8.52	9.35
	4404.75	1.557	−0.142	7.88	−13.40	−30.85	136	5	7.65	8.65
	4415.12	1.607	−0.615	7.93	−13.40	−31.34	106	5	7.63	8.63
	4433.21	3.653	−0.700	7.95	−13.40	−30.00	106	3	9.07	9.94
	4454.38	2.831	−1.250	7.97	−13.40	−31.60	57	5	8.21	9.10
	4459.11	2.175	−1.279	8.38	−13.40	−31.01	94	4	8.43	9.40
	4469.37	3.653	−0.260	8.08	−13.40	−30.00	96	2	8.46	9.31
	4484.21	3.602	−0.720	8.16	−13.40	−30.29	72	5	8.44	9.28
	4494.56	2.197	−1.260	8.38	−13.40	−31.01	100	3	8.54	9.50
	4531.14	1.484	−2.155	0	0	1.00	48	3	8.07	9.04
	4547.84	3.546	−0.780	0	0	1.00	55	4	8.19	9.03
									⟨8.23⟩	⟨9.14⟩
Fe II										
$\log\epsilon_\odot$	4202.52	6.807	−2.333	0	0	1.00	50	3	8.90	8.95
= 7.51	4250.43	7.683	−1.746	0	0	1.00	62	2	9.08	9.09
	4273.31	2.704	−3.340	8.54	0	1.00	143	4	9.13	9.47
	4286.31	7.708	−1.622	0	0	1.00	81	3	9.33	9.39
	4303.16	2.704	−2.490	8.54	0	1.00	142	3	8.23	8.61
	4314.28	2.675	−3.477	0	0	1.00	126	3	8.98	9.37
	4369.40	2.778	−3.670	8.45	0	1.00	118	3	9.00	9.38
	4384.09	6.225	−2.280	0	0	1.00	57	3	8.62	8.72
	4384.31	2.657	−3.500	8.44	0	1.00	104	3	8.45	8.83
	4385.38	2.778	−2.570	0	0	1.00	187	5	9.19	9.56
	4416.81	2.778	−2.600	8.54	0	1.00	162	5	8.67	9.03
	4431.62	7.940	−1.767	0	0	1.00	54	4	9.11	9.11
	4446.24	5.956	−2.439	0	0	1.00	67	4	8.80	8.94
	4448.52	11.149	−0.595	0	0	1.00	31	4	9.22	9.03
	4451.97	11.255	−0.742	0	0	1.00	25	2	9.27	9.07
	4461.43	2.582	−4.114	0	0	1.00	80	2	8.51	8.89
	4491.40	2.855	−2.700	8.45	0	1.00	96	5	7.60	7.97
	4499.70	7.693	−1.865	0	0	1.00	69	4	9.35	9.38
	4555.89	2.828	−2.290	0	0	1.00	118	3	7.64	8.04
	4576.33	2.844	−3.040	0	0	1.00	121	5	8.47	8.87
	4582.83	2.844	−3.100	0	0	1.00	114	4	8.38	8.77
									⟨8.74⟩	⟨8.97⟩

Table 2. (Continued.)

Element Solar ε	λ (Å)	χ (eV)	$\log gf$	$\log g_{\rm rad}$	$\log C_4$	$\log C_6$	W_λ (mÅ)	Weight	$\log \varepsilon$ adopted	$\log \varepsilon$ 9500 K
Ni I										
$\log \epsilon_\odot$	4401.54	3.193	0.080	0	0	0	30	3	6.27	7.08
= 6.25	4470.48	3.399	−0.400	0	0	0	28	5	6.84	7.64
									⟨6.63⟩	⟨7.43⟩
Sr II										
$\log \epsilon_\odot$	4215.52	0.000	−0.170	8.30	−12.74	0.47	190	1	3.41	4.47
= 2.9									⟨3.41⟩	⟨4.47⟩
La II										
$\log \epsilon_\odot$	4322.51	0.172	−1.640	0	0	0	42	3	4.00	5.07
= 1.22	4333.74	0.172	−0.170	0	0	0	57	1	2.80	3.91
	4559.29	0.772	−1.720	0	0	0	45	2	4.53	5.57
									⟨3.98⟩	⟨5.04⟩
Ce II										
$\log \epsilon_\odot$	4195.82	0.559	−1.340	0	0	0	30	5	4.53	5.47
= 1.55	4223.88	0.529	−1.170	0	0	0	15	2	3.95	4.88
	4248.68	0.683	−0.060	0	0	0	46	5	3.65	4.58
	4255.78	0.703	−0.270	0	0	0	44	2	3.83	4.76
	4257.12	0.459	−1.250	0	0	0	27	5	4.30	5.25
	4263.43	1.041	−0.440	0	0	0	42	2	4.20	5.11
	4268.30	0.736	−1.290	0	0	0	23	2	4.44	5.36
	4306.72	0.516	−0.380	0	0	0	47	2	3.86	4.81
	4367.00	1.365	−0.460	0	0	0	61	1	4.78	5.70
	4380.06	0.621	−1.140	0	0	0	47	2	4.67	5.62
	4393.19	0.740	−0.890	0	0	0	36	3	4.31	5.24
	4398.79	0.553	−0.970	0	0	0	31	4	4.15	5.10
	4399.20	0.326	−0.780	0	0	0	44	3	4.06	5.02
	4405.47	0.634	−1.340	0	0	0	31	4	4.58	5.52
	4418.78	0.863	0.030	0	0	0	41	1	3.56	4.50
	4439.24	1.365	−0.550	0	0	0	39	2	4.46	5.34
	4464.17	0.910	−1.180	0	0	0	38	2	4.74	5.67
	4486.91	0.295	−0.620	0	0	0	66	4	4.28	5.27
	4496.23	1.041	−0.660	0	0	0	53	4	4.59	5.52
	4519.59	1.347	−0.520	0	0	0	51	4	4.62	5.53
	4536.89	1.520	−0.430	0	0	0	31	4	4.28	5.15
	4560.96	0.683	−0.700	0	0	0	57	4	4.45	5.40
	4562.36	0.477	−0.070	0	0	0	70	3	3.92	4.91
									⟨4.28⟩	⟨5.22⟩
Pr II										
$\log \epsilon_\odot$	4222.93	0.054	0.130	0	0	0	40	3	2.99	4.24
= 0.71									⟨2.99⟩	⟨4.24⟩
Eu II										
$\log \epsilon_\odot$	4205.05	00	0.117	0	0	0	150	1	5.47	6.55
= 0.51	4405.27	2.090	−1.540	0	0	0	52	4	5.15	6.08
	4485.15	3.327	−0.340	0	0	0	63	3	5.01	5.86
									⟨5.14⟩	⟨6.06⟩

Table 2. (Continued.)

Element Solar ε	λ (Å)	χ (eV)	$\log gf$	$\log g_{\rm rad}$	$\log C_4$	$\log C_6$	W_λ (mÅ)	Weight	$\log \varepsilon$ adopted	$\log \varepsilon$ 9500 K
Gd II										
$\log \epsilon_\odot$	4225.15	0.600	−1.190	0	0	0	60	4	4.50	5.35
= 1.12	4310.98	0.492	−1.600	0	0	0	70	4	5.02	5.89
	4316.05	0.662	−0.660	0	0	0	104	3	5.03	5.96
	4316.27	1.133	−1.100	0	0	0	74	4	5.07	5.91
	4322.20	0.382	−1.540	0	0	0	61	4	4.69	5.56
	4324.06	1.133	−0.800	0	0	0	98	3	5.37	6.24
	4387.67	0.424	−1.370	0	0	0	87	2	5.12	6.03
	4426.15	0.382	−1.960	0	0	0	81	3	5.52	6.43
	4446.49	0.492	−1.710	0	0	0	70	3	5.10	5.97
	4483.33	1.060	−0.700	0	0	0	75	4	4.60	5.44
	4486.35	2.311	0.010	0	0	0	56	4	4.38	5.11
	4498.28	0.427	−1.430	0	0	0	61	5	4.58	5.46
									⟨4.87⟩	⟨5.73⟩

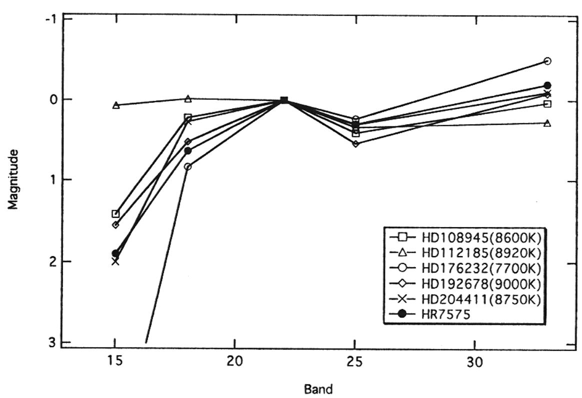

Fig. 2. UV fluxes of HR 7575 and magnetic stars. The flux units are magnitudes normalized to zero at band 22.

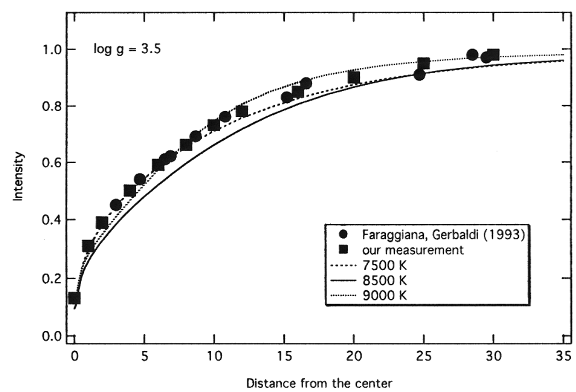

Fig. 3. The Hγ line profiles of HR 7575.

et al. (1973) for 10-times the solar composition models. The profiles measured on the tracing by Faraggiana and Gerbaldi (1993) for HR 7575 are also included in the figure. The model of $T_{\rm eff}$ = 8500 K fails to reproduce the observed profiles. Although a lower or higher temperature model of $T_{\rm eff}$ = 7300 K or 9500 K is preferable, these temperatures are not compatible with the values derived in subsection 3.1. When a larger surface gravity of $\log g = 4.0$ is chosen, the theoretical profiles deviate fairly from the observations compared with those for $\log g = 3.5$. That is, the model of $\log g = 3.5$ permits a better match to the effective temperatures obtained above. Faraggiana and Gerbaldi (1993) showed that the Hγ line profiles of HR 7575 resemble those of a cooler magnetic star β CrB ($T_{\rm eff}$, $\log g$, [M/H]) = (7750, 4.0, +0.5). However, the Hγ line profiles of HR 7575 are also found to be very similar to those of higher temperature stars, such as 73 Dra (A2p, Sr-Cr-Eu) and o Peg (A1 IV). A comparison of the Hγ line profile for 73 Dra gives $T_{\rm eff}$ = 9000 K, $\log g$ = 3.7 (Sadakane 1976), and Adelman (1988) obtained ($T_{\rm eff}$, $\log g$) = (9600, 3.60) for o Peg.

3.3. *Final Model Parameters*

By giving weight to the result of the optical energy distribution, we adopt $T_{\rm eff} = 8500 \pm 300$ K as the final effective temperature of HR 7575. This is very close to the value of 8650 K cited in the catalogue of Glagolevskij (1990). We can get an indication of $\log g$ for HR 7575 to be near 3.5 from the Hγ line profiles. An examination of the ionization temperature for Fe supports the choice of the surface gravity. It is found that when $\log g = 4.0$ is chosen, the ionization temperature will be 9700 K. This is greater by 450 K than that for $\log g = 3.5$ models and deviates greatly from the adopted effective temperature.

We use the ATLAS9 model atmosphere of ($T_{\rm eff}$, $\log g$, [M/H]) = (8500 K, 3.5, +1.0) in the following analysis.

4. Analysis

4.1. Microturbulent Velocity ξ

The microturbulent velocity ξ is obtained from the $\log \varepsilon$(Fe)–ξ relations for iron lines. They give 2.0 km s^{-1} for neutral lines, and 1.5 km s^{-1} for ionized lines. Finally, the following mean microturbulent velocity is adopted:

$$\xi = 1.75 \pm 0.5 \text{ km s}^{-1}. \tag{1}$$

We should note that it is very severe to find a unique microturbulent velocity. An estimation based on the requirement that the derived abundance be independent of the equivalent width gives different microturbulent velocities depending on the elements. For the Cr II, Fe I, and Fe II lines, $\xi = 0.0$ km s^{-1} seems to be acceptable. However, the Cr I and Ce II lines show $\xi = 1.75$ km s^{-1}, and a greater value is appropriate for Gd II. Ryabchikova et al. (1997) reported that the intrinsic microturbulence can be close to zero for the cool magnetic star γ Equ. They suggest that the magnetic field intensifies the lines due to the Zeeman effect, which mimics additional microturbulence. In the next section it will be shown that the absorption lines in HR 7575 are fairly intensified by the magnetic field. The unusual microturbulent velocities found in HR 7575 are possibly explained in the same way in γ Equ.

4.2. Abundance Computation

Elemental abundance computations were performed with WIDTH9, a companion program to the ATLAS9 (Kurucz 1993a). Damping constants were taken from Takeda (1984), and when no data were available in it, the internal approximations for damping in the WIDTH9 were used. The oscillator strengths were taken from Wiese and Martine (1980) for Mg II and Ca I, Martine et al. (1988) for Sc II, Ti II, and Cr I, Fuhr et al. (1988) for Fe I and Fe II, and ATMLINE database (Horaguchi, Hirata 1989) for heavier elements. When no gf values were found in the literature, Kurucz's (1994a, b, c) compilations were adopted for Ti II, Cr I, Cr II, Mn II, Fe I, and Fe II. For the Eu II line at λ4205.05, broadened heavily due to the hyperfine splitting (e.g., Biémont et al. 1982), the technique of spectrum synthesis was applied to obtain the equivalent width using the program SYNTHE (Kurucz 1993b).

The abundance results for each line are shown in table 2. The consecutive columns are the element (and solar abundance value), the wavelength λ, the lower excitation potential χ in eV, the $\log gf$ value, the radiative damping constant $\log g_{\rm rad}$; 0 means the adoption of the natural damping constant, the quadratic Stark damping constant (when no data was available, the internal form of WIDTH9 was chosen; it is indicated with 0), the van der Waals damping constant or the correction factor to the internal form of WIDTH9 (when its absolute value is less than 10, it is a logarithmic correction factor), the measured equivalent width W_λ, the weight (the highest weight 5 is given for very fine and unblended lines, and the lowest value 1 is for lines severely blended or broken) used at the final averaging of abundances, the computed abundance for the adopted effective temperature $T_{\rm eff}$ = 8500 K, and the abundance for the model of $T_{\rm eff}$ = 9500 K, which will be used to estimate the effect of the choice of models, respectively. Weighted mean abundances relative to those of the Sun are presented in brackets for each element.

4.3. Ionization Equilibria of Cr and Fe

As can be seen from tables 2 and 4, the iron abundance derived from neutral lines is lower by 0.50 dex than that from ionized iron lines. A higher effective-temperature model of $T_{\rm eff}$ = 9250 K is necessary to achieve an ionization balance for iron. For Cr, the abundances deduced from both ionic species yield the same value at $T_{\rm eff}$ = 8300 K, which is consistent with the adopted effective temperature.

4.4. Excitation Equilibria of Cr and Fe Lines

The second inconsistency in the results of the adopted model atmosphere is that the derived abundances depend on the lower excitation potential. To bring the abundances deduced from individual lines with various excitation potentials into agreement, a significantly higher temperature model of $T_{\rm eff}$ = 10000 K is preferable for both Cr and Fe.

5. Line Intensifications by the Magnetic Field

The magnetic field of up to 4000 G on HR 7575 is exceptionally strong among the cool CP stars (Didelon 1984). The influence of the magnetic field can be seen, for instance, in the Fe II lines at 4385.38 Å and 4416.81 Å. These lines have been studied in detail by Takeda (1991) as a line pair that is suitable for searching stellar magnetic fields. They belong to the same multiplet, and their gf values are essentially the same, while their effective Landé factors Z (position of the gravity center of the sigma components; Babcock 1962) are different. Therefore, the difference in the observed line strengths is expected to give the effect of the magnetic field. The present result for HR 7575 certainly shows the line at

Table 3. List of the lines selected to estimate magnetic intensifications.

λ(Å)	Transition	Z	W_λ	$\log\varepsilon$	W_λ^*	$\log\varepsilon^*$	$\Delta\varepsilon$
Cr I							
4262.38	a $^3G_3$–y $^3H^o_4$	0.875	26	7.91	22	7.81	0.10
4459.73	b $^5D_3$–w $^5F^o_4$	1.125	61	7.88	48	7.67	0.21
4492.31	b $^3P_2$–y $^3S^o_1$	1.250	60	7.84	44	7.59	0.25
Cr II							
4224.85	b $^2D_{3/2}$–z $^2P^o_{3/2}$	1.066	91	7.55	66	7.04	0.51
4275.57	a $^4F_{5/2}$–z $^4D^o_{3/2}$	0.900	142	7.67	120	7.19	0.48
4592.09	b $^4F_{5/2}$–z $^4D^o_{5/2}$	1.200	172	7.77	116	6.69	1.08
Fe I							
4202.02	a $^3F_4$–z $^3G^o_4$	1.150	102	7.62	72	7.05	0.57
4219.36	a $^1H_5$–y $^3I^o_6$	1.083	85	7.84	70	7.58	0.26
4404.75	a $^3F_3$–z $^5G^o_4$	1.250	136	7.65	106	7.13	0.52
4415.12	a $^3F_2$–z $^5G^o_3$	1.167	106	7.63	79	7.13	0.60
4454.38	b $^3P_2$–x $^3D^o_2$	1.333	57	8.21	42	7.97	0.24
4484.21	g $^5D_4$–z $^5P^o_3$	1.250	72	8.44	54	8.14	0.30
Fe II							
4385.38	b $^4P_{1/2}$–z $^4D^o_{1/2}$	1.333	187	9.19	123	8.05	1.14
4416.81	b $^4P_{1/2}$–z $^4D^o_{3/2}$	0.833	162	8.67	110	7.73	0.94
4491.40	b $^4F_{3/2}$–z $^4F^o_{3/2}$	0.400	96	7.60	92	7.52	0.08
4576.33	b $^4F_{5/2}$–z $^4D^o_{5/2}$	1.200	121	8.47	80	7.61	0.86

*Equivalent widths and logarithmic abundances after applying the correction for magnetic intensification.

4385.38 Å (187 mÅ, $Z = 1.333$) to be stronger than the line at 4416.81 Å (162 mÅ, $Z = 0.833$). This suggests that the magnetic intensifications due to Zeeman broadening should be taken into account to evaluate intrinsic elemental abundances.

5.1. *Abundances versus the Effective Landé Factors Z*

We present an additional examination of magnetic intensifications in figure 4, in which the Fe and Cr abundances are displayed as a function of the computed effective Landé factors Z. Their abundances, except for Fe I, increase with the effective Landé factor. This trend is the same as a result of, for instance, Kupka et al.'s (1996) demonstration (figure 1 of their paper) for the iron lines of the rapidly oscillating Ap star α Cir (HR 5463).

5.2. *Abundance Change due to the Magnetic Field*

To estimate more explicitly the influence of the magnetic field to the elemental abundances, we solve the Unno–Beckers equation, which describes the transfer of the Zeeman line radiation in the presence of a magnetic field. It was first formulated by Unno (1956) and revised by Beckers (1969) to include the magneto-optical effect. The equation in terms of the Stokes parameters (I, Q, U, V) is expressed under the condition of the local thermodynamic equilibrium (LTE) as follows (van Ballegooijen 1987):

$$\mu\frac{d}{dx}\begin{pmatrix} I \\ Q \\ U \\ V \end{pmatrix} = -\begin{pmatrix} \kappa_c+\kappa_I & \kappa_Q & \kappa_U & \kappa_V \\ \kappa_Q & \kappa_c+\kappa_I & \rho_V & -\rho_U \\ \kappa_U & -\rho_V & \kappa_c+\kappa_I & \rho_Q \\ \kappa_V & \rho_U & -\rho_Q & \kappa_c+\kappa_I \end{pmatrix} \times \begin{pmatrix} I \\ Q \\ U \\ V \end{pmatrix} + \begin{pmatrix} \kappa_c S_c + \kappa_I S_L \\ \kappa_Q S_L \\ \kappa_U S_L \\ \kappa_V S_L \end{pmatrix}, \tag{2}$$

where S_L and S_c are the line and continuum source functions; κ_c is the continuum opacity; $\kappa_I, \kappa_Q, \kappa_U$, and κ_V are the line opacities in each polarization mode; ρ_Q, ρ_U, and ρ_V describe magneto-optical effects; μ is the direction cosine of a ray; and x is the geometrical depth measured from the stellar surface. Unlike the opacities appearing in the transfer equation of unpolarized light, the κ's and ρ's are generally dependent on the angle of the magnetic field to the line of sight and on the azimuthal angle of the magnetic field.

We assume that both the continuum and the line spectrum will be formed under the condition of LTE. Then, the source function of S_L and S_c can be expressed as the Planck function B for black-body radiation, so that equation (2) will be reduced to a function of x if we choose

Table 4. Abundance comparison.*

Elment	This study $\Delta \log \varepsilon$	This study $\Delta \log \varepsilon^{\dagger}$	Allen (1977)	Allen, Cowley (1977)	Sun $\log \varepsilon$	Cool Ap stars $\Delta \log \varepsilon$
Mg II	0.01 (1)				7.58	−0.10
Ca I	0.78 (5)				6.36	0.46
Sc II	−0.02 (2)				3.10	0.02
Ti II	0.77 (18)				4.99	−0.32
Cr I	2.36 (23)	2.02			5.67	1.00
Cr II	2.24 (20)	1.30		1.36 (12)	5.67	1.00
Mn I	1.59 (1)				5.39	1.59
Mn II	2.10 (11)			1.96 (16)	5.39	1.59
Fe I	0.72 (27)	−0.01	−0.23 (39)		7.51	0.71
Fe II	1.23 (21)	0.22	0.06 (16)	0.24 (12)	7.51	0.71
Ni I	0.38 (2)				6.25	0.95
Sr II	0.51 (1)		1.94 (3)		2.90	1.98
Y II	—		−0.16 (8)		2.24	0.39
Zr II	—		0.85 (12)		2.60	
La II	2.76 (3)				1.22	
Ce II	2.73 (23)				1.55	
Pr II	2.28 (1)				0.71	
Eu II	4.63 (3)				0.51	
Gd II	3.75 (12)				1.12	

Notes:
*Model parameters (T_{eff}, $\log g$, ξ) are as follows: This study = (8500, 3.5, 1.75); Allen (1977) = (8000, 4.0, 3.5); Allen, Cowley (1977) = (8000, 4.0, 3.5).
†The relative abundance to the Sun after applying the correction for magnetic intensification.

some model atmosphere. As an initial condition, we assume that $I = S_{\mathrm{L}} = S_{\mathrm{c}} = B$, and $Q = U = V = 0$ at a fairly deep layer.

Equation (2) is solved by adopting the lambda operator method (Rees, Murphy 1987), where we also assume that $\mu = 0$ (that is, disk center), the angle of the magnetic field to the line of sight is 45°, the azimuthal angle of the magnetic field is arbitrary, and the Zeeman splitting patterns are described by the LS coupling.

The background continuum opacities, the line opacities, and the ionization degrees of the atomic elements are computed using a simple code written by one of the authors (K. K.) with the help of Mihalas (1967).

We select a total of 16 clean Cr and Fe lines (weight = 5) from table 2 to compute their intensity profiles I at a disk center under the condition of the presence of a magnetic field of 4000 G. Here, we consider the specific intensity at a disk center to be equivalent to the flux from the stellar surface. From a theoretical viewpoint, although the stellar spectra should be reproduced by integrating the specific intensity over a stellar disk, it is presently impossible for HR 7575, because of a lack of information concerning the geometrical structure of the magnetic field.

The Zeeman-broadened profiles are repeatedly simulated by solving the equation to reproduce the measured line strengths. Thus, we obtain abundances for the case of no magnetic intensification, which are compared in table 3 with those computed directly from the measured equivalent widths. The consecutive columns in table 3 are the wavelength, the term designation, the effective Landé factor (Z; computed on the assumption of LS coupling), the measured equivalent width W_λ, the logarithmic abundance $\log \varepsilon$ computed from this equivalent width, the equivalent width W_λ^* expected for the case of no magnetic intensification, the abundance $\log \varepsilon^*$ derived from W_λ^*, and the abundance difference between the two cases, respectively.

The final mean iron abundances for the case of no magnetic intensification are 7.50 and 7.73 for Fe I and Fe II, respectively, which are consistent with the recent solar value of 7.51 (Holweger et al. 1995; Blackwell et al. 1995; Anstee et al. 1997). On the other hand, after a correction of the effect of magnetic broadening, the Cr abundances are still greater than the solar value, ranging from 2.02 dex (Cr I) to 1.30 dex (Cr II), as revealed by tables 3 and 4.

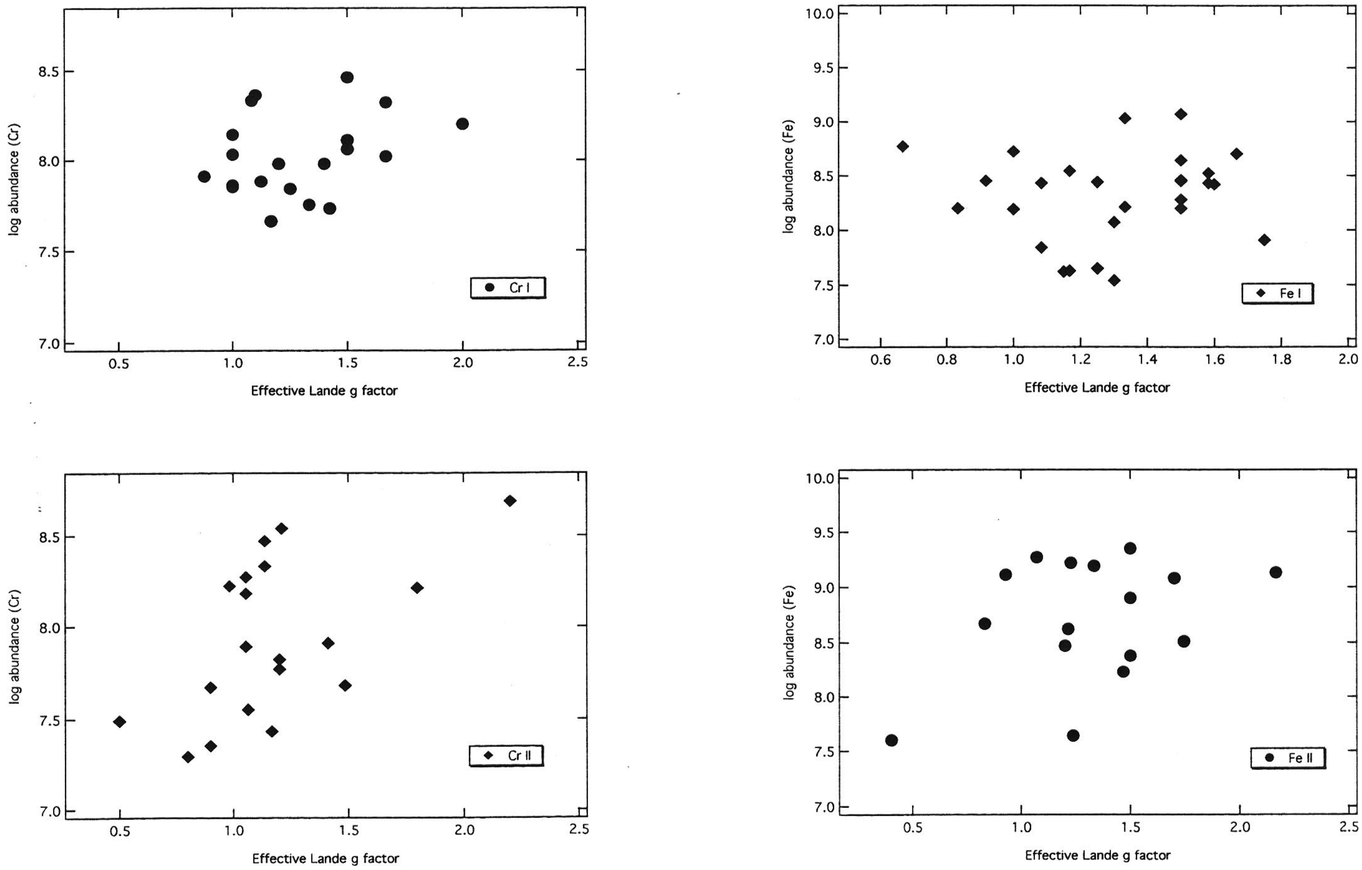

Fig. 4. Elemental abundances versus the effective Landé factors for Fe and Cr.

6. Discussion

6.1. Abundance Comparison

We summarize the final abundance results (the magnetic intensification is not taken into account) together with those of previous studies (Allen 1977; Allen, Cowley 1977) in table 4 and in figure 5, where the mean abundances for cool Ap stars are taken from Adelman and Cowley (1986), the solar abundances are from Anders and Grevesse (1989), and the solar iron abundance is from Holweger et al. (1995). The number of lines employed for each element is in parentheses. The second and third columns are the mean relative abundances deduced from tables 2 and 3, respectively. The final abundance result (no correction of the magnetic intensification) is displayed in figure 5, corresponding to the adopted model parameters ($T_{\rm eff} = 8500$ K, $\log g = 3.5$, $\xi = 1.75$ km s^{-1}, [M/H] $= +1.0$).

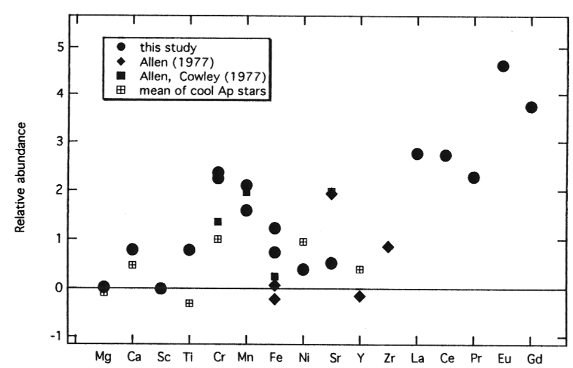

Fig. 5. Chemical composition of HR 7575 relative to the Sun in logarithmic units. The influence of Zeeman broadening is not taken into account.

The abundances of Mg and Sc presented here are solar, while Ca, Ti, Fe (derived from neutral lines), Ni, and Sr are slightly enhanced by 0.4–0.8 dex. Cr, Mn, and rare earth elements (La, Ce, Pr, Eu, and Gd) have abundances far greater than the solar values: they are highly enriched by 2.0–4.6 dex. Thus, the overall abundance pattern of HR 7575 is consistent with the mean values of cool CP stars (Adelman, Cowley 1986), except for Ti and Cr, which are greater by 1 dex than the means.

The elemental abundances in this study are systematically larger than those of Allen (1977) and Allen and Cowley (1977) by 0.14 to 1.17 dex, except for Sr. Our result for Sr is smaller than that of Allen (1977). We note that the Sr II line at 4215.52 Å is very sensitive to the choice of the damping constants. If we adopt an internal damping form of the WIDTH9 program, the Sr abundance will increase by 0.80 dex. The discrepancy in the abundances between Allen and us can be partly explained by the differences in the analysis method, model parameters, atmospheric models, and line parameters. In particular, a higher microturbulent velocity of $\xi = 3.50$ km s^{-1}by Allen (1977) yields lower abundances for all elements by 0.5 dex compared with the case of $\xi = 1.75$ km s^{-1}.

6.2. *Abundances Derived from Mathys' (1991) Equivalent Widths*

Mathys (1991) has measured two Cr II lines, four Fe I lines, and three Fe II lines lying between 5871 Å and 6380 Å for HR 7575. With their equivalent widths, the abundances of Cr and Fe were computed for the adopted model atmosphere of $T_{\rm eff} = 8500$ K. The resulting abundances are 8.46 for Cr, 8.70 and 9.22 for Fe, which are systematically larger than our present results by 0.5 dex. The temperature at which the Fe I and Fe II lines yield equal abundances is 9100 K. This is higher by 600 K than the adopted effective temperature, and well match to our ionization equilibrium temperature of 9250 K.

6.3. *Ionization Equilibria of Cool Magnetic CP Stars*

In order to examine the reliability of the breakdown in ionization equilibrium (see, subsection 4.3), we tried to recompute the abundances of Cr and Fe for four magnetic CP stars (HD 8441, HD 2453, 73 Dra, β CrB) by replacing the gf values, damping constants, model atmospheres, and the abundance computation code with those employed in this study. The equivalent widths for HD 8441 (A2 Sr), HD 2453 (A1 SrEuCr), 73 Dra (A2 SrCrEu), and β CrB (A9 SrEuCr) were taken from Adelman (1984), Adelman (1973), and Sadakane (1976), respectively. The resultant temperatures necessary to achieve ionization equilibria are given in table 5. Since the microturbulent velocities are not explicitly given for HD 2453 and β CrB, the abundance computations were made for two velocities.

Table 5. Ionization equilibrium temperatures for five magnetic CP stars.

Star	HD	SP	$B-V$	ξ	Cr	Fe
	8441	A2 Sr	+0.01	0.80	9800	9650
	2453	A1 SrEuCr	+0.06	1.50	9000	9650
				3.00	8970	9150
73 Dra	196502	A2 SrCrEu	+0.07	2.50	9100	8400
HR 7575	188041	A6 SrCrEu	+0.19	1.75	8300	9250
β CrB	137909	A9 SrEuCr	+0.27	1.50	7950	8500
				3.00	7950	8200

A fairly large temperature splitting ($\Delta T_{\rm eff} = 700$ K) in ionization equilibria is found only in 73 Dra.

We have anticipated that the ionization equilibrium temperatures would be different for each element in magnetic stars, because the magnetic intensifications depend on the property of the atomic structure of individual elements. However, it is impossible to conclude from these samples that the temperature splitting is a general phenomenon in magnetic CP stars.

7. Conclusion

In this analysis the following model paramaters are adopted: $T_{\rm eff} = 8500 \pm 300$ K, $\log g = 3.5$, the microturbulent velocity $\xi = 1.75 \pm 0.5$ km s^{-1}, and 10-times the solar metal content.

An effective temperature of 8500 ± 300 K is determined from the flux distributions.

The adopted surface gravity is a result of compromise choosing. An inspection of the Hγ line profiles implies that the surface graivity $\log g$ may be smaller than 3.5.

An uncertainty remains in the microturbulent velocity. It seems to depend on the individual elements.

Most of the lines are intensified by the strong magnetic field. By solving the Unno–Beckers equation, the abundances change due to the Zeeman broadening, which is estimated to be from 0.1 to 1.1 dex for Cr and Fe.

The elemental abundances of 17 species were obtained by an LTE model atmosphere analysis. Of the analyzed elements, Mg and Sc have nearly solar abundances, while Cr, Mn, and rare earths are overabundant by 1 to 5 dex. The most important result is a breakdown of the ionization balance between Fe I and Fe II.

We applied in this study the usual method of model atmosphere analysis to the magnetic CP star HR 7575. However, we failed to consistently perform the analysis because of peculiarities appearing in the Hγ line profile, in the microturbulence, in the ionization balance of Fe, in the excitation equilibria of Cr and Fe, and in the magnetically broadened spectrum lines. Further improved model atmospheres applicable to the magnetic stars are needed for more reliable abundance studies.

We wish to thank Dr. C. R. Cowley and the staff at the Dominion Astrophysical Observatory for their hospitality. We also appreciate Dr. R. L. Kurucz for kindly sending us a CD-ROM set containing the ATLAS9 model atmospheres.

References

Adelman S.J. 1973, ApJS 26, 1
Adelman S.J. 1981, in Upper Main Sequence Chemically Peculiar Stars (Université de Liège, Belgium) p13
Adelman S.J. 1984, A&A 141, 362
Adelman S.J. 1988, MNRAS 230, 671
Adelman S.J., Cowley C.R. 1986, in Upper Main Sequence Stars with Anomalous Abundances, IAU Coll. No.90, ed C.R. Cowley, M.M. Dworetsky, C. Mégessier (D. Reidel, Dordrecht) p305
Adelman S.J., Pyper D.M., Shore S.N., White R.E., Warren W.H.Jr 1989, A&AS 81, 221
Allen M.S. 1977, ApJ 213, 121
Allen M.S., Cowley C.R. 1977, PASP 89, 386
Anders E., Grevesse N. 1989, Geochim. Cosmochim. Acta 53, 197
Anstee S.D., O'Mara B.J., Ross J.E. 1997, MNRAS 284, 202
Babcock H.W. 1954, ApJ 120, 66
Babcock H.W. 1958, ApJS 3, 141
Babcock H.W. 1960, in Stellar Atmospheres, ed J.L. Greenstein (University of Chicago Press, Chicago) p282
Babcock H.W. 1962, in Astronomical Techniques, ed W.A. Hiltner (University of Chicago Press, Chicago) p107
Beckers J.M. 1969, Sol. Phys. 9, 372
Biémont E., Karner C., Meyer G., Träger F., zu Putlitz G. 1982, A&A 107, 166
Blackwell D.E., Lynas-Gray A.E., Smith G. 1995, A&A 296, 217
Breger M. 1976, ApJS 32, 7
Buscombe W. 1977, MK Spectral Classifications, Third General Catalogue (Northwestern University, Evanston)
Catalano F.A., Renson P. 1984, A&AS 55, 371
Cowley C.R. 1976, ApJS 32, 631
Cowley C.R. 1977, ApJ 213, 451
Cowley C.R. 1979a, in Spectral Classification of the Future, IAU Coll. No.47, ed M.F. McCarthy, A.G.D. Philip, G.V. Coyne (Vatican Observatory) p375
Cowley C.R. 1979b, ApJS 39, 429
Cowley C.R. 1993, in Peculiar versus Normal Phenomena in A-type and Related Stars, IAU Coll. No.138, ed M.M. Dworetsky, F. Castelli, R. Faraggiana, ASP Conf. Ser. 44, p18
Cowley C.R., Aikman G.C.L. 1980, ApJ 242, 684
Cowley C.R., Aikman G.C.L., Fisher W.A. 1977, Publ. Dom. Astrophys. Obs. 15, 37
Didelon P. 1983, A&AS 53, 119
Didelon P. 1984, A&AS 55, 69
Faraggiana R. 1989, A&A 224, 162
Faraggiana R., Gerbaldi M. 1993, in Peculiar versus Normal Phenomena in A-type and Related Stars, IAU Coll. No.138, ed M.M. Dworetsky, F. Castelli, R. Faraggiana, ASP Conf. Ser. 44, p169
Faraggiana R., Gerbaldi M., Castelli F., Floquet M. 1986, A&A 158, 200
Fuhr J.R., Martine G.A., Wiese W.L. 1988, J. Phys. Chem. Ref. Data 17, Suppl. 4
Glagolevskij Yu.V. 1990, in Hot Chemically Peculiar and Magnetic Stars, ed G. Scholz (Academy of Sciences of the GDR, Potsdam) p43
Hartoog M.R., Cowley C.R., Cowley A.P. 1973, ApJ 182, 847
Hauck B., Mermilliod M. 1980, A&AS 40, 1
Hauck B., North P. 1982, A&A 114, 23
Hauck B., North P. 1993, A&A 269, 403
Hoffleit D. 1982, The Bright Star Catalogue, 4th ed (Yale University Observatory, New Haven)
Holweger H., Kock M., Bard A. 1995, A&A 296, 233
Horaguchi T., Hirata R. 1989, ATMLINE: Relational Database of Atomic Spectral Lines, Data Processing Center, Kyoto Univ., Bulletin 22, 129 (in Japanese)
Jones T.J., Wolff S.C. 1973, PASP 85, 760
Kato K., Sadakane K. 1993, Publ. Sci. Mus. Osaka 3, 1 (Science Museum of Osaka, Osaka)
Kodaira K. 1967, Ann.Tokyo Astron. Obs. II, 10, 157
Kodaira K. 1973, A&A 26, 385
Kupka F., Ryabchikova T.A., Weiss W.W., Kuschnig R., Rogl J., Mathys G. 1996, A&A 308, 886
Kurucz R.L. 1993a, ATLAS9 Stellar Atmosphere Programs and 2km/s Grid, Kurucz CD-ROM No.13 (Smithsonian Astrophysical Observatory, Cambridge, MA)
Kurucz R.L. 1993b, SYNTHE Spectrum Synthesis Programs and Line Data (Kurucz CD-ROM No.18; Smithsonian Astrophysical Observatory, Cambridge, MA)
Kurucz R.L. 1994a, Atomic Data for Ca, Sc, Ti, V, and Cr (Kurucz CD-ROM No.20; Smithsonian Astrophysical Observatory, Cambridge, MA)
Kurucz R.L. 1994b, Atomic Data for Mn and Co (Kurucz CD-ROM No.21; Smithsonian Astrophysical Observatory, Cambridge, MA)
Kurucz R.L. 1994c, Atomic Data for Fe and Ni (Kurucz CD-ROM No.22; Smithsonian Astrophysical Observatory, Cambridge, MA)
Lebedev V.S. 1987, AZh 64, 1308 = SvA 316, 686
Lester J.B., Gray R.O., Kurucz R.L. 1986, ApJS 61, 509
Martine G.A., Fuhr J.R., Wiese W.L. 1988, J. Phys. Chem. Ref. Data 17, Suppl. 3
Mathys G. 1990, A&A 232, 151
Mathys G. 1991, A&AS 89, 121
Mathys G., Cowley C.R. 1992, A&A 253, 199
Mathys G., Lanz T. 1992, A&A 256, 169
Mihalas D. 1967, in Astrophysics, Method in Computational Physics 7, ed B. Alder, S. Fernbach, M. Rotenberg (Academic Press, New York) p1
Mégessier C. 1988, A&AS 72, 551
Musielok B. 1986a, Acta Astron. 36, 131
Musielok B. 1986b, in Upper Main Sequence Stars with Anomalous Abundances, IAU Coll. No.90, ed C.R. Cowley, M.M. Dworetsky, C. Mégessier (D. Reidel, Dordrecht) p179
Musielok B., Lange D., Schöneich W., Hildebrandt G., Želwanowa E., Hempelmann A., Salmanov G. 1980, Astron. Nachr. 301, 71
Musielok B., Madej J. 1988, A&A 202, 143
Osawa K. 1965, Ann. Tokyo Astron. Obs. II, 9, 123
Preston G.W. 1971, ApJ 164, 309
Preston G.W. 1974, ARA&A 12, 257
Rees D.E., Murphy G.A. 1987, in Numerical Radiative Transfer, ed W. Kalkofen (Cambridge University Press) p241
Ryabchikova T.A. 1991, in Evolution of Stars: The Photospheric Abundance Connection, IAU Symp. 145, ed G.

Michaud, A. Tutukov (Kluwer Academic Publishers, Dordrecht) p149
Ryabchikova T.A., Adelman S.J., Weiss W.W., Kuschnig R. 1997, A&A 322, 234
Sadakane K. 1976, PASJ 28, 469
Schöneich W. 1981, in Upper Main Sequence Chemically Peculiar Stars (Université de Liège, Belgium) p235
Shallis M.J., Baruch J.E.F., Booth A.J., Selby M.J. 1985, MNRAS 213, 307
Shallis M.J., Blackwell D.E. 1979, A&A 78, 48
Smalley B., Dworetsky M.M. 1995, A&A 293, 446
Stępień K., Dominiczak R. 1989, A&A 219, 197
Takeda Y. 1984, PASJ 36, 149
Takeda Y. 1991, PASJ 43, 823
Thompson G.I., Nandy K., Jamar C., Monfils A., Houziaux L., Carnochan D.J., Wilson R. 1978, Catalogue of Stellar Ultraviolet Fluxes (UK Science Research Council)
Unno W. 1956, PASJ 8, 108
van Ballegooijen A.A. 1987, in Numerical Radiative Transfer, ed W. Kalkofen (Cambridge University Press) p279
Vidal C.R., Cooper J., Smith E.W. 1973, ApJS 25, 37
Warren W.H.Jr 1973, AJ 78, 192
Wesselius P.R., van Duinen R.J., de Jonge A.R.W., Aalders J.W.G., Luinge W., Wildeman K.J. 1982, A&AS 49, 427
Wiese W.L., Martine G.A. 1980, Wavelength and Transition Probabilities for Atoms and Atomic Ions, NSRDS-NBS 68 (US Government Printing Office, Washington DC)
Wolff S.C. 1969, ApJ 158, 1231
Wolff S.C. 1983, The A-Type Stars: Problems and Perspectives, NASA SP-463 (NASA, Scientific and Technical Information Branch, Washington DC)